

# Study of relaxation rates of stable paramagnetic centers in $\gamma$ -irradiated alanine

B. Rakvin <sup>a,\*</sup>, N. Maltar-Strmečki <sup>b</sup>

<sup>a</sup> Ruder Bošković Institute, PO Box 1016, 10001 Zagreb, Croatia

<sup>b</sup> The Faculty of Veterinary Medicine, University of Zagreb, Zagreb, Croatia

Received 10 June 1999; accepted 17 September 1999

## Abstract

The stable L-alanine radical induced by  $\gamma$ -irradiation was examined by electron paramagnetic resonance (EPR), transfer saturation EPR and electron nuclear double resonance (ENDOR) in the temperature region of fast motion of the methyl group (180–320 K). From the obtained spectral line broadening and spectral intensity the correlation time for the methyl rotation was estimated. The complex processes determining the relaxation rate were examined in the same temperature interval. It was shown that important contributions to the relaxation rate arise from non-secular and pseudo-secular types of contributions. The non-secular contribution involves intramolecular dynamics while the pseudo-secular contribution originates from intermolecular motions. The obtained values for the dynamical parameters have been compared with those obtained by pulse EPR methods and by proton nuclear magnetic resonance (NMR) on undamaged crystals. © 2000 Elsevier Science B.V. All rights reserved.

*Keywords:* L-alanine; Paramagnetic centers; Electron paramagnetic resonance; Spin-lattice relaxation time

## 1. Introduction

Electron paramagnetic resonance (EPR) spectra of irradiated alanine currently employed in alanine/EPR dosimetry [1,2] exhibit a complex spectroscopic structure. The latter is mainly due to the unresolved hyperfine structure and motional averaging effects of electron proton hyperfine couplings. From single crystal studies two major radical species can be expected at room temperature. The first one is the so-called ‘stable alanine

radical’ (SAR1) with the well established spectroscopic parameters and the second one is the so-called ‘second stable radical’ (SAR2) with spectroscopic parameters which have recently been reported [3].

Electron spin-lattice relaxation times,  $T_1$ , obtained by various pulse and nonlinear techniques on L-alanine centers also reveal more than one single relaxation rate [4,5]. One expects that the EPR intensities and saturation factors of these centers could strongly depend on the spectral diffusion mechanism. Indeed, it was demonstrated [4] that in the continuous wave (CW) saturation experiment, the dominant relaxation rate is due to

\* Corresponding author. Fax: +385-1-4680245.

E-mail address: rakvin@faust.irb.hr (B. Rakvin)

the spectral diffusion mechanism and not due to the usually expected spin-lattice relaxation mechanism.

Knowledge of the detailed temperature dependence of the relaxation rates may have important implication for alanine/EPR dosimetry [6]. The signal/noise ratio of the alanine spectrum can be enhanced by about 30% by recording the EPR spectrum at the maximum relaxation rate at about 200 K as compared to room temperature. This enhancement might be of great significance in the therapy-level dose range where the detected signal is very small and comparable to the background signal.

It is well known that the SAR1 linewidths and spectral intensities are modulated by the rotational rate of the methyl groups. However, a dynamic parameter such as the correlation time for the rotation of the methyl group,  $\tau$  which is essential for deducing this particular relaxation mechanism, is not well defined, and can be found in literature in a wide range of time scales [7–11]. Despite of numerous studies with different EPR techniques, the Arrhenius behavior of the correlation time has been described with energy barriers,  $\Delta E/k$ , lying in a large energy interval from 1100 K to 2400 K and with an even more uncertain pre-exponential value,  $\tau_\infty$  lying inside an interval of two orders of magnitudes (0.1–0.001 ps).

The relaxation rate of the SAR1 center was studied by employing several CW-EPR [7], electron nuclear double resonance (ENDOR) [9] and pulse EPR techniques [5,8]. Besides that several characteristic relaxation times were detected [4,5], the origin of the corresponding relaxation mechanisms was not completely clear. For example,  $T_1$  measured by various pulse EPR techniques on the SAR1 center [5] leads to two or even three different  $T_1$ 's. In these studies, for all suggested models of relaxation,  $\tau$  is involved as the most important parameter. On the other hand, a more accurate estimation of  $\tau$  could help to evaluate various relaxation mechanisms that contribute to the relaxation rate in a wide temperature interval. In order to obtain more accurate  $\tau$  values of the methyl group in SAR1 the temperature dependence of the CW-EPR spectrum was reinvestigated in the fast motional region of the methyl

group (180–320 K). The present study was undertaken because one expects that the EPR spectrum in this particular temperature interval exhibits the most intense changes due to the motional dynamics of methyl group, leading to a more precise measurement of  $\tau$ .

In this work, EPR, CW-Transfer Saturation EPR (CW-TSEPR) and ENDOR techniques have been employed to study the methyl dynamics in the temperature region around the maximum relaxation rate. The results are compared with  $\tau$  of methyl groups obtained earlier for SAR1 [7–9] and with the methyl group dynamics measured by proton nuclear magnetic resonance (NMR) in non-irradiated samples [12].

## 2. Experimental

Single crystals of L-alanine were grown by slow evaporation from a D<sub>2</sub>O solution at room temperature. The crystals were irradiated by  $\gamma$ -rays from <sup>60</sup>Co source with a dose of 10 kGy. EPR, CW-TSEPR and ENDOR spectra were obtained by using a Varian E109 with home made ENDOR facilities. Stanford research system (SRS844 and SRS830) lock-in amplifiers with high range of frequency modulation 1 mHz–250 MHz and simultaneous in-phase and out-of-phase (also called phase quadrature) detection facilities have been employed. These units are connected to a PC that simultaneously provides data acquisition.

Transfer saturation spectra were recorded as the second harmonic of the modulation frequency absorption signal. The possibility to employ a wide range of modulation up to 250 MHz gives an additional opportunity to detect out-of-phase signals with much faster relaxation rates than in the usual cases when a lock-in amplifier with 100 kHz modulation is employed.

## 3. Results

The spectroscopic parameters of the EPR spectrum of SAR1 are well described and the spectrum can be easily resolved in the temperature range 180–300 K [3]. In order to study relaxation

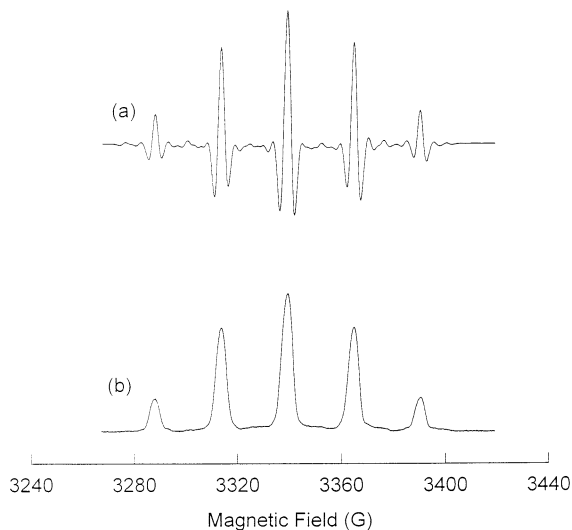


Fig. 1. Experimental EPR spectra from an  $\gamma$ -irradiated L-alanine single crystal at room temperature with the magnetic field along the  $c$  axis at (a) absorption spectrum at the second harmonic in-phase with a magnetic field modulation of 50 kHz; and (b) absorption spectrum at the second harmonic out-of-phase (quadrature signal) with a magnetic field modulation of 50 kHz.

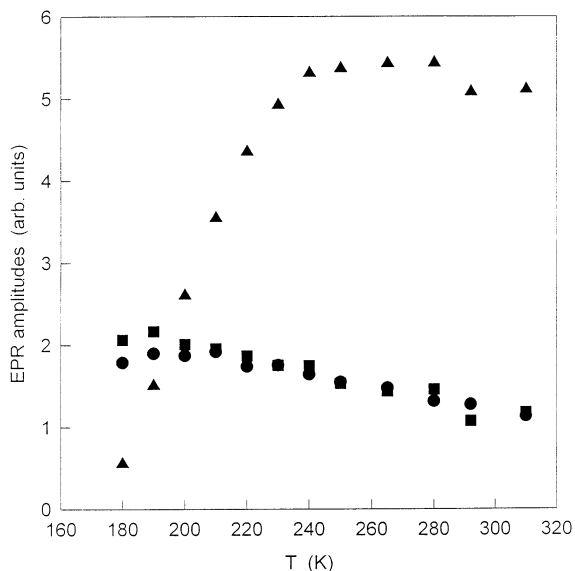


Fig. 2. Temperature dependence of the EPR peak amplitudes for the sextet (triangles), low field singlet (circles) and high field singlet (squares) of L-alanine single crystal spectra detected at the second harmonic in-phase with 50 kHz modulation frequency. The spectra were recorded at low microwave power (0.1 mW).

rate for this center the orientation of the crystal in the magnetic field ( $B$ ),  $B \parallel c$  with the simplest form of the SAR1 spectrum as a quintet (1:4:6:4:1) line intensities will be employed. Fig. 1a shows the L-alanine quintet detected at the second harmonic in phase with 50 kHz modulation frequency. The dominant structure of the spectrum originates from three equivalent  $\beta$ -protons and one  $\alpha$ -proton with an almost identical splitting. The effect of methyl proton dynamics as a function of temperature is seen as the broadening (decreasing in amplitude) of the central sextet line in comparison to the outer singlets which remain nearly unchanged. These changes in the L-alanine spectrum were described by modified Bloch equations and the correlation time of proton motion was deduced [7]. It should be noted here that the model of the modified Bloch equations only considers changes in  $\tau$  and spin-spin relaxation time,  $T_2$ , without taking into account any contributions from  $T_1$  to the linewidth. As was shown in ref. [7]  $\tau$  was obtained by fitting the whole quintet spectrum. However, one can also deduce  $\tau$  simply by measuring the line-broadening contribution to the linewidth of the central line in comparison to the outer singlet linewidths. In the fast motional region this can be approximated in the following form:

$$\Delta\Gamma = \Gamma_{se} - \Gamma_{si} \quad (1a)$$

$$\Delta\Gamma_{exp} = \frac{(\Gamma_{sil} + \Gamma_{sih})}{2} \left( \sqrt[3]{\frac{3(Y''_{sil} + Y''_{sih})}{Y''_{se}}} - 1 \right) \quad (1b)$$

$$\Delta\Gamma_{exp} \approx c\tau = c\tau_{\infty} e^{\frac{\Delta E}{kT}} \quad (1c)$$

Here  $\Gamma_{sil}$ ,  $\Gamma_{sih}$  and  $\Gamma_{se}$  represents the half linewidth at half intensity for the singlet at low and high field and the sextet line respectively.  $Y''$  represent the amplitude for these lines detected at the second harmonic. The average value of the singlets was employed for  $\Gamma_{si}$  in order to reduce possible contributions from the  $\alpha$ -proton splitting. It is convenient to calculate a line-broadening contribution to the linewidth from relation (Eq. (1b)) at the temperature where the amplitude of the sextet is equal to the amplitude of the singlet. Fig. 2 shows the typical temperature dependence of the amplitudes for the two singlet and sextet

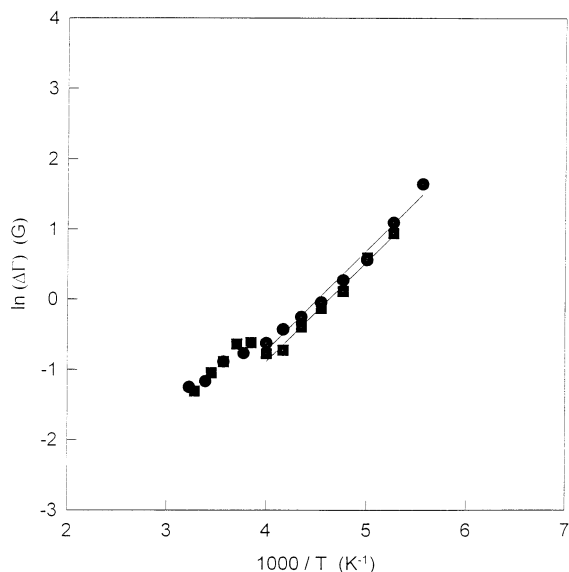


Fig. 3. Temperature dependence of the logarithm of the sextet line-broadening contributions for L-alanine spectra detected at the second harmonic in-phase with a modulation frequency of 500 Hz (circles) and 1 MHz (squares). The spectra were taken at low microwave power (0.1mW). The solid line represents a linear fit to the experimental data in the low temperature region (180–240 K).

lines detected at the second harmonic of 50 kHz modulation. By employing relation (Eq. (1c)) at the crossing point of these amplitudes one can deduce  $\tau$  for the constant of proportionality ( $c_B = 4.107 \times 10^9$ , for  $\Delta\Gamma$  expressed in gauss) which was calculated from the modified Bloch equations [7] and including correction [8]. By knowing  $\tau$  at the temperature of the crossing point and the activation energy in the vicinity region of this tempera-

ture, the  $\tau_\infty$  value can be also deduced from relation (1). Fig. 3 shows a logarithmic plot of the sextet broadening versus  $1/T$  for spectra recorded at 0.1 mW of microwave power (below saturation of SAR1 [5]) and at different modulation frequencies (500 Hz and 1 MHz). The expected Arrhenius behavior of the sextet broadening can be seen for both plots in the low temperature region (180–240 K), while a deviation from this behavior appears at higher temperatures (240–320 K). Spectra in the low temperature region were used to deduce  $\tau$  and the temperature of the crossing point. These results are given in Table 1.

Besides the already discussed typical L-alanine quintet spectrum detected in-phase (Fig. 1a) a quadrature spectrum in the same conditions is shown in Fig. 1b. It can be noted that for the quadrature spectrum an integral absorption line shape (not the second derivative as the in-phase signal) is obtained. This type of quadrature signal is typical for rapid passage mode (RPM) [13]. In general, one expects that a quadrature signal contains information on species (or spin packets) with less microwave saturation than the species (or spin packets) which contribute to an in-phase signal. In the simple temperature dependent experiment it can be seen that the typical quintet quadrature spectrum detected at 200 K exhibits a different height ratios than one detected in-phase at the same temperature. In order to make an easier comparison, a quadrature spectrum is derived and an in-phase signal was integrated (Fig. 4). The smaller ratio between the height of the central line and the outer singlet lines in the quadrature spectra, as compared with the same

Table 1

Parameters for correlation times and temperatures of the crossing point of amplitude for the sextet and outer singlets obtained at different modulation frequencies and microwave powers

| Microwave power (mW) | Modulation frequency (kHz)                             |                                                        |                                                        |                                                        |
|----------------------|--------------------------------------------------------|--------------------------------------------------------|--------------------------------------------------------|--------------------------------------------------------|
|                      | 0.5                                                    | In-phase 50                                            | Out of phase 50                                        | 1000                                                   |
| 0.1                  | $T_{cr} = 195$ K ( $E/k = 1554$ K ( $\zeta = 0.058$ ps | $T_{cr} = 195$ K ( $E/k = 1590$ K ( $\zeta = 0.048$ ps |                                                        | $T_{cr} = 192$ K ( $E/k = 1562$ K ( $\zeta = 0.049$ ps |
| 20                   |                                                        | $T_{cr} = 195$ K ( $E/k = 1517$ K ( $\zeta = 0.069$ ps | $T_{cr} = 212$ K ( $E/k = 2158$ K ( $\zeta = 0.006$ ps |                                                        |

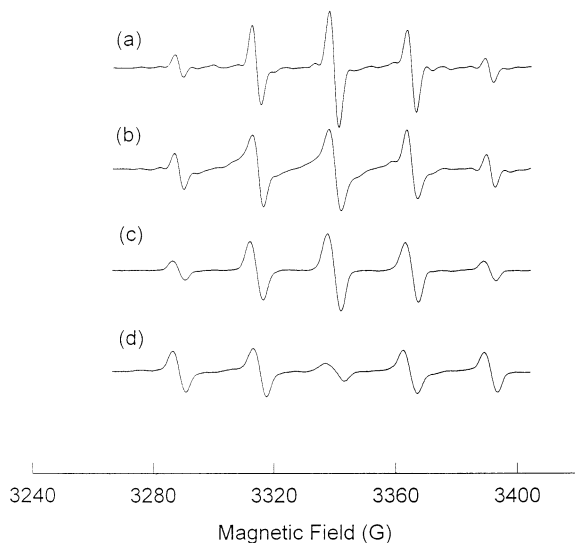


Fig. 4. EPR in-phase and quadrature spectra of L-alanine detected under the same condition as described in Fig. 1. The in-phase spectrum was integrated to reach the first derivative lineshape (a) at 295 K and (c) at 200 K. The quadrature spectrum was derivated to reach the first derivative lineshape (b) 295 K and (d) 200 K. The figure illustrate the changes in ratio of the signal heights between the sextet and the outer singlets for in-phase and quadrature spectra at low temperature.

ratios for the in-phase spectra clearly indicate different relaxation behavior for the two types of spectra. Fig. 5 shows the contribution to the line broadening for the in-phase and quadrature spectra by employing a microwave power of 20 mW in the examined temperature interval. Broadening of a sextet line for the in-phase spectra exhibit almost a straight line in the logarithm  $\Delta\Gamma$  versus  $1/T$  plot. It can be noted that broadening behavior for the in-phase spectra detected at 20 mW almost coincide with broadening of the in-phase spectra but recorded at low microwave power (0.1 mW). In the similar plot broadening of the quadrature spectra exhibit a deviation from the straight line of in-phase spectra contributions at higher and lower temperatures. Deviation from Arrhenius behavior suggests that an additional relaxation time is involved in the relaxation mechanism. Indeed, the estimated relaxation times at temperatures of the crossing amplitudes exhibit a larger activation energy for the quadrature spec-

tra than the activation energy detected for the in-phase spectra (Table 1). A significant difference in the temperatures of the crossing points for the quadrature and in-phase spectra can also be noted.

As was discussed earlier the ENDOR intensity of SAR1 strongly depends on the cross-relaxation rate [9]. For this study a L-alanine crystal was oriented with the magnetic field along *a* axis. ENDOR intensity and linewidth for the line near 48 MHz were detected at the high field EPR singlet as a function of temperature. Because of the sensitivity of the signal on phase modulation in this experiment the magnitude spectrum was detected [13,14] at the second harmonic of 100 kHz modulation frequency. Fig. 6 shows the natural logarithm of the ENDOR intensity (squares) and linewidth (circles) as a function of  $1/T$ . The expected extremal behavior of the ENDOR intensities can be observed with a maximum intensity in the vicinity of 250 K. The obtained linewidths

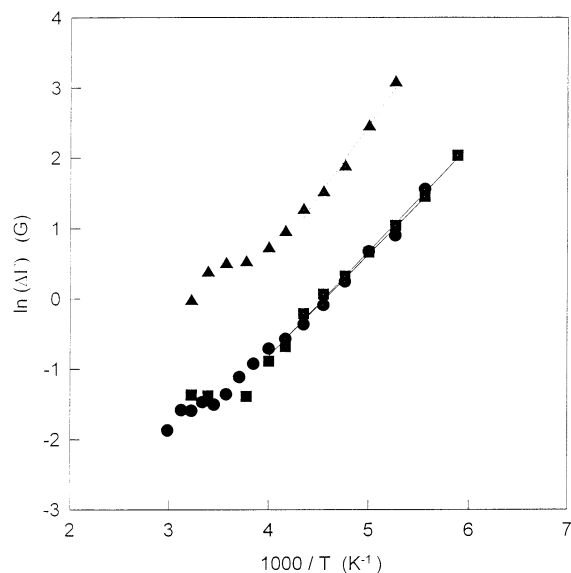


Fig. 5. Temperature dependence of the logarithm of the sextet line-broadening contributions for L-alanine spectra detected at second harmonic in-phase with a modulation frequency of 50 kHz and a microwave power of 0.1 mW (squares), 20 mW (circles) and 20 mW for the quadrature spectrum (triangles). The solid line is the best linear fit in the temperature interval (180–240 K) and the dotted line is the best fit in the temperature interval (200–240 K).

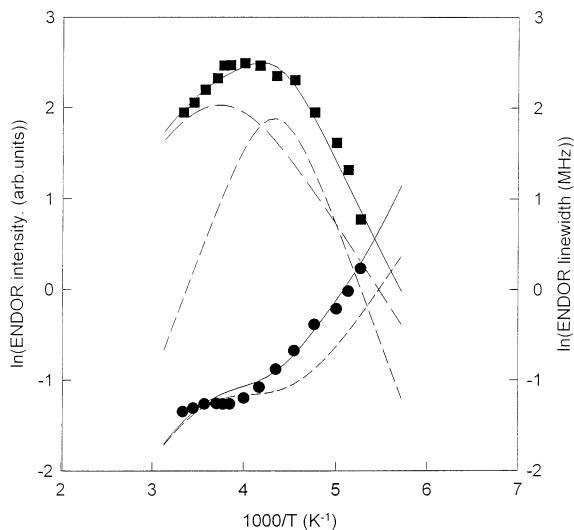


Fig. 6. Temperature dependence of the logarithm of the ENDOR intensity (squares) and ENDOR linewidth (circles) obtained at the high field singlet of the L-alanine EPR spectrum. The ENDOR spectra were recorded as magnitude spectra at the second harmonic of the magnetic field modulation (100 kHz). The dashed line (top-left) represents the non-secular contribution from relation (Eq. (2)). The dashed line (top-right) represents pseudo-secular contribution and the solid line (top) represents the cumulative contribution. The dashed line (bottom) represents the calculated linewidth from relation (Eq. (3)) without the pseudo-secular contribution and the solid line (bottom) represents the linewidth calculated from relation (Eq. (3)).

and intensities are similar to previous experiments [9] except that they exhibit a slightly broader distribution on the temperature scale.

#### 4. Discussion

These experiments clearly demonstrate that despite of the presence inhomogeneously broadened lines in the spectrum the detected broadening of the central line in comparison to the external singlet lines leads to a relaxation mechanism which exhibits Arrhenius behavior. This behavior can be found for all spectra detected with a small microwave power regardless of the modulation frequency in the low temperature region. Fig. 2 shows that the largest rate of change for the sextet amplitudes is observed in the low temperature

region. Therefore, the deduced  $\Delta E/k$  in this temperature region exhibits a relatively high accuracy (within 2% of error). The obtained  $\Delta E/k$  is smaller (around 150 K) than the  $\Delta E/k$  evaluated earlier [7] having an error of 5.5%. The reason for these discrepancies is the deviation from Arrhenius behavior at higher temperatures. It was shown that the size of this deviation depends on the microwave power and the phase detection of the signal. The improved accuracy in  $\Delta E/k$  also gives a more accurate value for  $\tau_\infty$  as shown in Table 1.

The detected deviation from the simple Arrhenius behavior exhibits extremal behavior with a small maximum around 280 K. Presence of maxima in the temperature dependence of the line-broadening contribution indicates that an additional relaxation mechanism is involved, which would contain non-secular or pseudo-secular types of relaxation terms. For such a mechanism the non-secular term of the relaxation mechanism related to the cross-electron-nuclear-relaxation ( $\Delta M_S + \Delta M_I = 0$ ) was detected as an effective relaxation mechanism in the examined temperature interval [9]. A maximum in the relaxation rates can be expected when  $\tau 2\pi\nu_0 \cong 1$ , where  $\nu_0 \approx 9.5$  GHz for the non-secular terms, and  $\nu_0 \approx 14.5$  MHz for the pseudo-secular term respectively. The ENDOR method suggested earlier [9], is convenient for efficient detection of the cross-relaxation contribution from the intensity of the ENDOR line. The intensities of the ENDOR lines exhibit extremal behavior with a maximum around 250 K (Fig. 6). On the other hand, the position of the maximum at the temperature scale can be calculated from  $\tau$  (Table 1). One can calculate the position of the maximum by taking  $\tau$  from the EPR parameters for a modulation frequency 0.5 kHz (Table 1) and denoted as  $\tau_B$ . At the maximum of the relaxation rate for 9.5 GHz one can calculate the position of the maximum at 274 K. The obtained disagreement is too large to be neglected and the contribution of the cross-relaxation detected by EPR is not in agreement with the ENDOR experiment. However, it can also be seen (Figs. 3, 5 and 6) that the maximum of the line-broadening contribution detected by EPR near 280 K, coincides with a deviation in the

ENDOR line behavior. Therefore, the non-secular relaxation mechanism could be responsible for the deviation from the Arrhenius behavior in the higher temperature region if an additional relaxation mechanism is also active in the lower temperature region.

The deviation from Arrhenius behavior can be minimized by decreasing the microwave power and by employing a phase sensitive detection. This is clearly seen in Fig. 5 where at different phase detections, line-broadening contributions exhibit Arrhenius behavior or extremal behavior for the same temperature interval.

A quadrature signal is a non-linear effect and can not be simply analytically described [13]. However, these types of spectra are sensitive to  $T_1$  relaxation processes and motional diffusion which is in the order of  $T_1 \sim \omega_m^{-1} \sim \tau$ . Therefore, without a detailed simulation of the quadrature, spectrum it is difficult to separate contribution from the possible motional diffusion or  $T_1$  relaxation rates. Only qualitatively it can be noted that a non-secular type of mechanism contribute in the high temperature region. The clearer and larger intensity of the maximum around 280 K than in other detected broadening contributions supports the assumption that the non-secular relaxation rate with the same  $\tau_B$  is involved in relaxation mechanism of the quadrature signal. However, the larger  $\Delta E/k \approx 2158$  K of the quadrature signal in the low temperature region compared to the in-phase signal indicates that additional motional dynamics contribute to the relaxation rate. Since there is not a clear maximum, as in the high temperature region, the origin of this mechanism cannot be simply deduced.

As can be seen from the above considerations at least two different relaxation mechanisms can be separated by employing CW-EPR and CW-TSEPR techniques. Since the contributions of these mechanisms can be obscured by the inhomogeneous nature of the CW spectra, an ENDOR or pulse EPR method, which reduce this effect, can be employed for more detailed studies. Therefore, in order to check the obtained parameters for the correlation times, the ENDOR method was employed to obtain intensities of the SAR1 lines in the same temperature interval. It

was shown [9] that the ENDOR line intensity is proportional to:

$$E \propto \frac{w_x}{w_e}$$

$$w_x \approx \frac{1}{2} j(\omega_e)$$

$$j(\omega_e) = \frac{b^2}{8} \frac{\tau}{(1 + \tau^2 \omega_e^2)} \quad (2)$$

Here,  $w_e$  is the electron transition probability,  $w_x$  is the electron-nuclear-cross probability,  $j(\omega_e)$  is the spectral density and  $b$  is the coupling constant [9]. By employing relation (Eq. (2)) and  $\tau_B$  one can describe only a part of the experimental results in Fig. 6 as shown by the dashed line (left line on the top in Fig. 6). However, this maximum coincides with a deviation of the ENDOR line-broadening in the high temperature region. According to the previous consideration [9] the residual ENDOR linewidths can be approximated as:

$$\Gamma_{\text{ENDOR}} \approx \frac{1}{2\pi T_2}$$

$$= \frac{1}{2\pi} \frac{1}{4} ((j(0) + 7j(\omega_e)) + (j_n(0) + j_n(\omega_n))) \quad (3)$$

Here, the last two terms represent possible pseudo-secular contributions. The temperature dependence of  $\Gamma_{\text{ENDOR}}$  was described only by the first two terms in [9]. By using this description and with the known values for  $b/2\pi = 140$  MHz and  $\tau_B$ ,  $\Gamma_{\text{ENDOR}}$  is presented as the dashed line in Fig. 6 (bottom line). Similarly, as in previous work [9], a good qualitative agreement can be seen especially for the expected position of the non-secular contribution in the high temperature region. An additional misfit should be ascribed to the neglecting of the dipolar and other inhomogeneous contributions. The quadrature spectra indicate that an additional  $\tau$  with higher potential barrier should be considered in the low temperature region. Therefore, it can be supposed that neighbor methyl groups of the radical centers, which exhibit small splittings in the order of a few MHz [15], are described with a  $\tau$  which is coupled to the

lattice dynamics. Indeed,  $\tau_n$  ( $\tau_\infty = 0.09$  ps,  $\Delta E/k = 2710$  T) corresponding to the methyl group motion measured by proton NMR on the undamaged crystal [12] can be employed in relation (Eq. (3)). In order to better describe the ENDOR linewidths, the relation (Eq. (3)) is employed and besides  $b$ ,  $\tau_B$  and  $\tau_n$  only one constant was adjusted in  $j_n$  ( $b/33$ ) leading to a solid line in Fig. 6 (bottom line). The employed constant ( $b/33$ ) leads to a small proton hyperfine coupling ( $((b/2\pi)/33) \approx 2.1$  MHz) which is expected for a next neighbor group. This agreement indicates that for the ENDOR line intensities a similar pseudo-scalar term ( $j_n(\tau_n\omega_n)$ ) should be added to relation (Eq. (2)). In this case  $\tau_B$ ,  $\tau_n$ , and two coupling constants ( $b$ ,  $b/27$ ) are applied and the continuous line with fairly good agreement is obtained as a sum of the two processes. Here, the temperature dependence of  $\omega_e$  was neglected as in the original model [9]. It can be noted that the ratios between coupling constants in both processes (33, 27) are comparable supporting the same origin of these pseudo-secular relaxation mechanisms. As was demonstrated here, besides that small hyperfine coupling, the contribution of the pseudo-secular mechanism (especially around the maximum of relaxation rate,  $\tau_n\omega_n \approx 1$ ) to the integral relaxation rate can be significant. The obtained qualitative fit of the ENDOR experimental data also supports the origin of the high potential barrier detected for quadrature signals in the low temperature region.

Another alternative to the described ENDOR intensities is to assume that only a single  $\tau$  is present. The obtained parameters for the unique  $\tau$  ( $\tau_\infty \approx 0.005$  ps,  $\Delta E/k \approx 2050$  K) [9] lead to a large decrease in the pre-exponential factor and an increase in the energy barrier in comparison to  $\tau_B$ . It should be mentioned that according to proton NMR measurements of non-irradiated L-alanine, the pre-exponential factor is not shorter than 0.09 ps. The increase of  $\tau_\infty$  can only reach  $\sim 1$  ps for methyl groups in various amino acids with the variation of hydrogen-bond densities. One cannot expect that a local potential in the vicinity of SAR1 center will change so drastically that the pre-exponential factor decreases with nearly two orders in magnitude with a simultaneous small

decrease in the energy barrier [16]. Therefore, it is more probable that an oversimplified description of the relaxation mechanism leads to this discrepancy.

An additional checking of the obtained  $\tau_B$  can be provided by analyzing multi-frequency data for  $T_1$  relaxation times of the SAR1 center measured at room temperature [5]. Two different  $T_1$  relaxation times are detected by the pulse saturation transfer method measured at various microwave frequencies. The possible origin of these relaxation mechanisms was discussed but there was no conclusive suggestion for it. In study [5], it was pointed out that the faster relaxing component in the recovery curves decreased with increased microwave frequency and the ratios of the weightings between this component and the slower component were evaluated for each frequency. One can suppose that the faster component corresponds to the cross-relaxation mechanism, dominant around room temperature. The ratio of the weightings of the short and long components (which were extrapolated at  $t=0$  in the pulse experiment) is proportional to the ratio of the corresponding transition probabilities. On the other hand, the ratio of the transition probabilities for the forbidden and allowed transitions is proportional to  $1/\omega_e^2$ . Therefore, one can expect that the ratio of weightings for these components is also proportional to  $1/\omega_e^2$  if the faster relaxation component is proportional to a cross-relaxation. Fig. 7a shows the experimentally obtained [5] ratios of weighting components as a function of frequency, and the fitted solid line on the  $1/\omega_e^2$  dependence. This leads to a functional dependence of the short component and supports the electron-nuclear-cross-relaxation as a relaxation mechanism. For a further check of the relaxation mechanism, one can expect that the relaxation rate for the cross-relaxation mechanism is proportional to  $j(\omega_e)$  and the relaxation time  $T_1^{\text{ef}}$  is proportional to:

$$T_1^{\text{ef}} \propto \frac{1}{b^2} \left( \frac{1}{\tau} + \tau\omega^2 \right) \quad (4)$$

Indeed, a good proportionality between the data for the relaxation times obtained in [5] and relation (Eq. (4)) (Fig. 7b) can be seen. From the

nonlinear fit the values of  $\tau = 0.113$  ps for the short component and  $\tau = 0.131$  ps for the long component are obtained. It can be noted that the fit for the short relaxation time is within the experimental error while the long relaxation time contains a larger error. This is expected since besides different non-secular types of contribu-

tions, which lead to a similar functional dependence, additional pseudo-secular contributions are not included in relation (Eq. (4)).

The obtained agreement between  $\tau$  deduced from the cross-relaxation mechanism measured by the frequency variation and  $\tau_B(295\text{ K}) = 0.112$  ps at room temperature gives a strong support to the accuracy of the  $\tau$  extracted from temperature dependent experiments by employing CW-EPR and ENDOR techniques.

## 5. Conclusion

It was shown that the reorientation of the methyl group in the SAR1 center can be also accurately studied by CW-EPR at minimum microwave power when using a wide frequency modulation range. The contribution of lattice dynamics through different reorientation rates of neighboring methyl groups was detected by employing CW-TSEPR and ENDOR techniques.

The presence of spin density on neighboring methyl group protons in principle complicates a full theoretical treatment of the relaxation rates for the SAR1 center. However, it is shown that besides this qualitative treatment, additional motional dynamics should be introduced in the relaxation mechanism. This can reduce discrepancies in dynamical parameters reported previously for the methyl dynamics of the SAR1 center.

## References

- [1] D.F. Regulla, U. Deffner, *Int. J. Appl. Radiat. Isot.* 33 (1982) 1101.
- [2] J.W. Nam, D.F. Regulla, *Appl. Radiat. Isot.* 40 (1989) 953.
- [3] E. Sagstuen, E.O. Hole, S.R. Haugedal, W.H. Nelson, *J. Phys. Chem. A* 101 (1997) 9763.
- [4] M. Brustolon, U. Segre, *Appl. Magn. Reson.* 7 (1994) 405.
- [5] B.T. Ghim, J.-L. Du, S. Pfenninger, G.A. Rinard, R.W. Quine, S.S. Eaton, et al., *Appl. Radiat. Isot.* 47 (1996) 1235.
- [6] B. Rakvin, *Appl. Radiat. Isot.* 47 (1996) 525.
- [7] I. Miyagawa, K. Itoh, *J. Chem. Phys.* 36 (1962) 2157.
- [8] S.A. Dzuba, K.M. Salikhov, D. Tsvetkov, *Chem. Phys. Lett.* 79 (1981) 568.

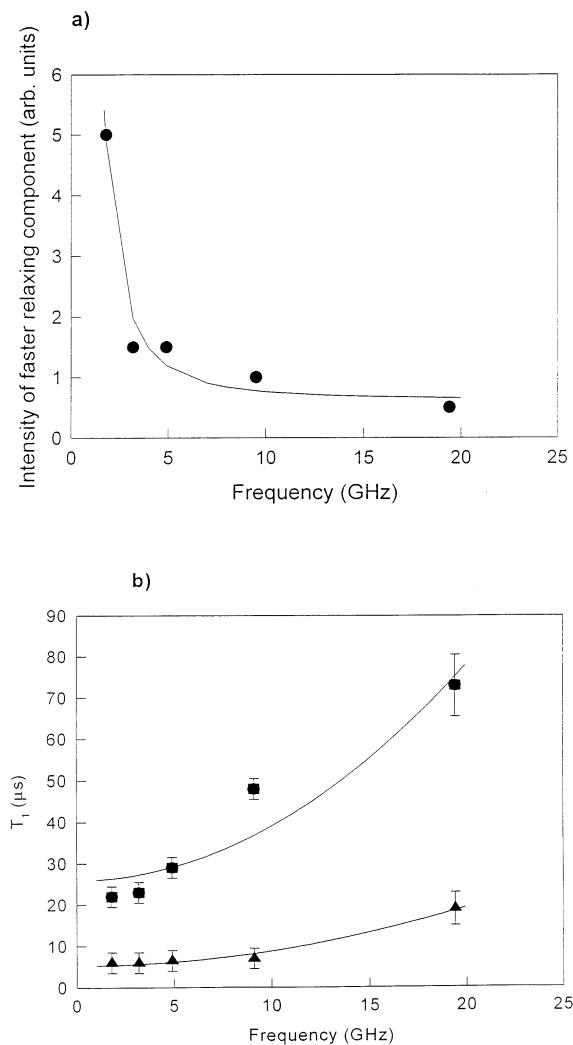


Fig. 7. (a) The experimental data for the frequency dependence of the faster relaxation component obtained from [5]. The solid line represents the best fit to  $1/\omega_c^2$ . (b) The experimental data for the frequency dependence of the long (squares) and the short (triangles) relaxation time obtained from reference [5]. The solid line corresponds to the best nonlinear fit of experimental values to relation (Eq. (4)).

- [9] M. Brustolon, T. Cassol, L. Micheletti, U. Segre, *Molec. Phys.* 57 (1986) 1005.
- [10] B. Rakvin, *Appl. Radiat. Isot.* 47 (1996) 1251.
- [11] R. Angelone, C. Forte, C. Pinzino, *J. Magn. Reson. A101* (1993) 16.
- [12] E.R. Andrew, W.S. Hinshaw, M.G. Hutchins, R.O.I. Sjöblom, P.C. Canepa, *Molec. Phys.* 32 (1976) 795.
- [13] L.R. Dalton, B.H. Robinson, L.A. Dalton, P. Coffey, Saturation transfer spectroscopy, advances in magnetic resonance 8, in: J.S. Waugh (Ed.), Academic Press, New York, 1976.
- [14] M.A. Hemminga, P.A. de Jager, Saturation transfer spectroscopy of labels, techniques and interpretation of spectra, in: L.J. Berliner, J. Rueben (Eds.), *Biological Magnetic Resonance 8*, Plenum Press, New York, 1989 (Chapter 3).
- [15] S. Kuroda, I. Miyagawa, *J. Chem. Phys.* 76 (1982) 3933.
- [16] A.R. Sørnes, N.P. Benetis, *J. Magn. Reson.* 125 (1997) 52.